Research Square

Preprints are preliminary reports that have not undergone peer review.
They should not be considered conclusive, used to inform clinical practice,
or referenced by the media as validated information.

Dual Modified Calcined Oyster Shell Lime Grouts for Crack Repair in Humid Coastal Limestone Relics

Yongguo Chen
Zhejiang University of Science and Technology
Miaodan He
Zhejiang University of Science and Technology
Jinyao Ye
Zhejiang University of Science and Technology
Liang Ye
liangye662162@163.com

Zhejiang University of Science and Technology
Shusheng Shen
Zhejiang University of Science and Technology
Sheng Ye
Zhejiang University of Science and Technology
Zixuan Chen
Zhejiang University of Science and Technology
Jinjing Chen
Zhejiang University of Science and Technology
Ruiqi Zhang
Zhejiang University of Science and Technology
Zhen Wang
Zhejiang University of Science and Technology
Yingzi Huang
Zhejiang University of Science and Technology
Yi Chen
Zhejiang University of Science and Technology

Article

Keywords: Calcined oyster shell lime, Grouting materials, Limestone heritage, SiO2 nanosol, Hydroxypropyl methylcellulose, Fissure repair, Highly humid coastal environment

Posted Date: November 10th, 2026

DOI: https://doi.org/10.21203/rs.3.rs-11373123/v1

License: This work is licensed under a Creative Commons Attribution 4.0 International License.
Read Full License

Additional Declarations: No competing interests reported.

Dual Modified Calcined Oyster Shell Lime Grouts for Crack Repair in Humid Coastal Limestone Relics

Yongguo Chen[a,b], Miaodan He[a], Jinyao Ye[a],Liang Ye[a,b,*], Shusheng Shen[a,b,*], Sheng Ye[c], Zixuan Chen[d],Jinjing Chen[a], Ruiqi Zhang[a],Zhen Wang[a], Yingzi Huang[a] and Yi Chen[a]

Abstract

Coastal humidity accelerates fissure deterioration of limestone artifacts, requiring grouts to combine substrate compatibility with environmental durability. Discarded oyster shells from Sanmen, Zhejiang were calcined as the sole binder, blended with silica fume and polycarboxylate superplasticizer, then modified with SiO_2 nanosol or hydroxypropyl methylcellulose at 0.2 to 0.6%. SEM and XRD revealed modification mechanisms, while grouting simulation and onsite repair at Hangzhou Yuewang Temple verified serviceability. The optimal 0.4% nanosol dosage coupled pozzolanic reaction with micro filling, generating calcium silicate hydrate gel and an acicular AFt skeleton, achieving nearly 11 and 10 MPa in 28 d compression and 1.8 MPa in flexure. At 0.4% dosage and low water to binder ratio, HPMC water retention cut shrinkage to 0.2 to 0.3% and raised 28 d bond strength from 0.2 to 0.65 MPa. Cracks deeper than 50 mm suit SSPSi systems, while 40 to 50 mm shallow cracks suit SSPSH systems.

Keywords：Calcined oyster shell lime；Grouting materials；Limestone heritage；SiO2 nanosol；Hydroxypropyl methylcellulose；Fissure repair；Highly humid coastal environment

1. Introduction

Stone cultural heritage carries nonrenewable historical information and remains vulnerable to cracking, hollowing, water seepage, and weathering. Once cracks are interconnected, they act as preferential pathways for moisture, soluble salts, and microorganisms, which in turn trigger salt crystallization, freeze thaw damage, and biodeterioration[1] . In coastal regions, the combined effects of climate change and the

marine environment make this issue particularly acute in coastal areas, and sea level rise, storm surges, and humidity fluctuations markedly accelerate the dissolution and salt weathering of carbonate stones [2, 3]. Grouting offers the most direct and effective means of sealing such cracks, although material selection is constrained by substrate compatibility and environmental durability. Grout strength and elastic modulus should stay close to those of the host stone, because excessive stiffness concentrates interfacial stress and induces secondary damage, whereas insufficient mechanical capacity weakens the reinforcement. Materials must likewise endure sustained high humidity, where excessive shrinkage leads to cracking and detachment and soluble salts provoke efflorescence and powdering[4]. Across southeastern coastal China, annual mean relative humidity frequently exceeds 70%, which alters grout hydration, carbonation, and moisture migration and this poses a more rigorous test of its operational reliability[5]. Consequently, developing grouts that simultaneously satisfy substrate compatibility and high-humidity durability has become a pressing bottleneck for the conservation of coastal stone heritage.

With this objective in mind, prior research has advanced along three paths. The first combines early-strength acceleration with internal curing. Montmorillonite and similar agents release interlayer adsorbed water, cutting the 7 day autogenous shrinkage of natural hydraulic(NHL) lime to 5.67% of the control and raising its 28 day compressive strength by 22.03% [6]. Studies of high ductility modification, domestic NHL substitution, and grout selection for detached murals further improved toughness and practical performance[7-9]. In 2026, Sarcinella and Frigione conducted a systematic review of approaches to the functional modification of phase-change energy storage materials in lime-based and naturally hydraulic lime mortars since 2010. They pointed out that, whilst such components improve the thermal performance of historic buildings, they must maintain good compatibility and long-term durability with the matrix, and outlined the trend towards multifunctional, integrated lime-based protective materials [10].Such admixtures, however, thicken the paste even as they accelerate hardening, so

injectability and full hydration rarely coexist. A second path turns to siliceous pozzolans. Among these, nano SiO_2 far exceeds powdered silica fume in pozzolanic reactivity owing to its fine particles and large specific surface. Fernández et al. showed that nano SiO_2 paired with a polycarboxylate superplasticizer cuts water demand while markedly strengthening lime mortars [11], and later work confirmed its stable pozzolanic contribution at later ages[12]. Yet how overdosage agglomeration, viscosity surge, and water to binder ratio coupling sway the balance between flowability and strength remains unquantified. The third path employs organic water retainers. Hydroxypropyl methylcellulose, for instance, forms a networked colloidal film that redirects moisture migration and raises water retention, with plastic viscosity rising in step[13]. The same film retards early hydration even as it curbs evaporation, leaving the threshold dosage at which its negative effects emerge undefined.

Binder selection is equally critical. For centuries, builders across southeastern coastal China calcined oyster shells into a calcium oxide rich and weathering resistant lime, a staple of historic construction in Fujian and Zhejiang[14]. Ranked among the three traditional hydraulic limes of ancient China, it has been characterized and modified alongside jiangshi and Aga earth[15-17], and Zhang et al. examined the factors governing its mortar performance[18].Several reviews have shown that the use of waste shells as aggregate or a cementitious component is technically feasible; however, an excessively high replacement rate may compromise mechanical and durability properties[19-23], and the influence of particle size on mortar transport has been quantified[24]. Concrete made with full oyster shell aggregate retains acceptable strength[25], A study by Terzić et al. published in Materials in 2026 assessed, through chemical and mineralogical analysis, the feasibility of using various solid waste materials—including calcium carbonate derived from oyster shells—as substitutes for natural limestone in the production of cement clinker. The study confirmed that, following calcination, such green raw materials can form a mineralogical composition similar to that of conventional clinker, thereby opening up a pathway for the resource

utilisation of calcium carbonate derived from oyster shells as a clinker substitute[26]; In 2026, Thang et al. conducted a series of mix design tests to quantify the effects of partially replacing natural sand with waste oyster shells on the workability and mechanical properties of mortar and concrete, noting that, within an appropriate substitution range, the engineering performance could meet the requirements for both structural and non-structural applications[27].while shell aggregate variability and the substitution potential of shell powder have been appraised [28]. Chen et al. modified traditional shell lime with metakaolin and doubled early strength while curbing shrinkage[29]. Bellei et al. partially replaced natural hydraulic lime with oyster shell powder or aggregate and kept property fluctuations below 10% after accelerated aging[30]. Calcined shell powder partially replacing slaked lime also yields viable ecological mortars[31]. Even so, shells appear almost exclusively as admixtures or aggregates below 30%. Systematic modification of calcined shell lime as the sole binder for grouting cracks in humid coastal limestone heritage therefore remains unexplored, as do the mechanistic contrast between inorganic nano silica sources and organic water retaining components, the criteria for mix selection, and the gap between standard laboratory curing and real substrates in actual climates [32].

To close these gaps, this work adopted calcined oyster shell lime from Sanmen, Zhejiang as the sole binder, blended it with silica fume and a polycarboxylate superplasticizer, and separately introduced SiO_2 nanosol and hydroxypropyl methylcellulose, forming the SSPSi and SSPSH dual modified series. Full factorial tests spanning water to binder ratios of 0.40 to 0.55, silica fume contents of 10% to 15%, and modifier dosages of 0.2% to 0.6% tracked setting time, fluidity, shrinkage, moisture content, water absorption, mass change, and mechanical performance at different curing ages. SEM and XRD observations clarified the modification mechanisms, while laboratory grouting trials and on site restoration at Yuewang Temple in Hangzhou assessed practical performance. To our knowledge, this study is the first to establish a dual modified grouting system built on calcined shell lime alone, one that separates the

chemical acceleration of nanosol from the physical water retention of hydroxypropyl methylcellulose under high humidity. It further resolves the microstructural evolution governed by coupled water to binder ratio and dosage effects, tying macroscopic behavior to hydration product morphology. Field verified rules linking crack depth to mix proportion selection offer coastal stone heritage projects a directly workable repair route based on locally sourced materials.

2. Materials and Methods

2.1 Experimental Materials

Oyster shell lime was prepared by calcining oyster shells collected from Sanmen County, Taizhou, Zhejiang Province, China, at approximately 900 °C. The calcined product was ground to 200 mesh and appeared pale white. Because lime derived from calcined shells is chemically analogous to carbonate rock artifacts and introduces no soluble salts, it is considered a suitable binder for the conservation of limestone cultural relics[33]. Silica fume was microsilica (SiO_2 content of 54.85%) supplied by Hebei Tangxian Xinlei Mineral Products Processing Plant. The polycarboxylic acid water-reducing agent is Shanxi Feike FK-A powder, with a water-reduction rate of 45 %.The SiO_2 nanosol was purchased from Guangzhou Fufei Chemicals; it is a neutral colloidal system with a SiO_2 content of 29.7%, an average particle size of 14.7 nm, a high specific surface area, and pozzolanic activity. Given that this nanosilica source has a small particle size and high reactivity, excessive incorporation can easily lead to agglomeration and impair workability; consequently, relevant studies generally limit its incorporation to a low range [34-36]. Hydroxypropyl methylcellulose (HPMC) is a product manufactured by Jingzhou Fuqiang Fine Chemicals; it has a fineness of 200 mesh and a viscosity of 200,000 mPa·s. Tap water was used for mixing. The chemical compositions of Oyster shell lime and silica fume are shown in Table 1, and the phase composition of Oyster shell lime is shown in Table 2.

Table1 Chemical compositions of OSL and SF (%)

Material	SiO_2	CaO	Al_2O_3	MgO	Fe_2O_3	K_2O	Na_2O
OSL	4.30	78.50	1.80	1.50	0.90	0.40	0.30
SF	54.85	37.42	3.07	3.78	0.12	0.44	0.32

Table2 Phase composition of OSL (%)

Phase	CaO	$Ca(OH)_2$	$CaCO_3$
Content	78.5	15.2	12.8

2.2 Instruments and Equipment

A Bruker D8-DISCOVER X-ray diffractometer (XRD), a Hitachi SU1510 scanning electron microscope equipped with energy-dispersive X-ray spectroscopy (SEM-EDS), an NLD-3 cement mortar flow tester, a Vicat apparatus (EN 196-3), a 101-2B electric forced-air oven, a DKZ-6000 electric cement flexural strength tester, an STYE-1000 hydraulic digital compression testing machine, and an HC-2000A bond strength tester were used in this study.

2.3 Mix Proportion Design

The following abbreviations are used throughout the text: a reference system comprising ground lime, silica fume and polycarboxylate superplasticizer; SS denotes the binary system of ground lime and silica fume, used for comparison of bonding performance; SSPS denotes the reference control group; SSPSi denotes the series incorporating SiO_2 nanosol; and SSPSH denotes the series incorporating HPMC. Specimen designations follow a three-part format: SSPSi12.5 0.50 0.4 denotes a silica fume content of 12.5 %, a water-to-binder ratio of 0.50, and a SiO_2 nanosol content of 0.4 %.

The experiments were conducted as a two-level factorial design. In the first level, the operational window was determined by the water-to-binder ratio and the silica fume content, with the silica fume content range based on the commonly used range for lime–siliceous pozzolan systems[37]; at the second level, silica sol or HPMC was introduced

at three dosage levels—0.2 %, 0.4 % and 0.6 %—into each of the five representative combinations screened out, forming two modified series, SSPSi and SSPSH, with an SSPS control group established to isolate the effects of the modifier itself. The specific proportions are shown in Tables 3.

Table3 Mix proportions of modified OSL-based cementitious materials

Sample No.	SF dosage (%)	W/B ratio	Modifier type	Modifier dosage (%)
SSPS (Control)	10.00 / 12.50 / 15.00	0.40~0.55	–	0
SSPSi12.5 0.4	12.50	0.40	Silica sol / HPMC	0.20 / 0.40 / 0.60
SSPSi10 0.45	10.00	0.45	Silica sol / HPMC	0.20 / 0.40 / 0.60
SSPSi10 0.5	10.00	0.50	Silica sol / HPMC	0.20 / 0.40 / 0.60
SSPSi12.5 0.5	12.50	0.50	Silica sol / HPMC	0.20 / 0.40 / 0.60
SSPSi15 0.55	15.00	0.55	Silica sol / HPMC	0.20 / 0.40 / 0.60
SSPSH12.5 0.4	12.50	0.40	Silica sol / HPMC	0.20 / 0.40 / 0.60
SSPSH10 0.45	10.00	0.45	Silica sol / HPMC	0.20 / 0.40 / 0.60
SSPSH10 0.5	10.00	0.50	Silica sol / HPMC	0.20 / 0.40 / 0.60
SSPSH12.5 0.5	12.50	0.50	Silica sol / HPMC	0.20 / 0.40 / 0.60
SSPSH15 0.55	15.00	0.55	Silica sol / HPMC	0.20 / 0.40 / 0.60

2.4 Sample Preparation and Curing

To ensure the uniformity of the slurries and comparability between the series, different addition sequences were adopted for the two modifiers: for the SSPSi series, the SiO_2 nanosol was first pre-dispersed in the mixing water before being blended with the cementitious materials; for the SSPSH series, the HPMC powder was first dry-mixed uniformly with the cementitious materials, followed by the addition of water and stirring. All slurries were mixed according to the following procedure: mixing at low speed for 120 s, stopping for 15 s, followed by mixing at high speed for a further 120 s, to eliminate silica sol stratification and HPMC agglomeration[38].

Upon completion of mixing, the slurry is poured into standard triple moulds measuring 40 mm × 40 mm × 160 mm and deaerated; given the high viscosity of the HPMC-modified slurry, the vibration time for the SSPSH series is appropriately extended to eliminate microscopic voids. After moulding, the surfaces are levelled and the specimens are numbered. After moulding, the specimens were demoulded and immediately transferred to a curing chamber maintained at a temperature of 20 ± 2 °C and a relative humidity of >70 %. This high-humidity environment was designed to simulate the actual conditions for the conservation of coastal limestone cultural heritage, ensuring that the hydration reaction proceeded fully and enabling the assessment of the material's suitability in the target environment. The specimens were cured for 7, 14 and 28 days, respectively, before being removed for testing.

2.5 Test Methods

Fluidity was determined in accordance with GB/T 2419-2005. After the mortar was compacted and levelled within a truncated conical mold, it was placed on a flow tester and subjected to 25 jolts, and the average of the expansion diameters in two mutually perpendicular directions was recorded. Setting time was determined using a Vicat apparatus according to GB/T 1346-2011. Shrinkage, moisture content, and water absorption were measured according to JGJ/T 70-2009. Mass changes were monitored using an electronic balance to track the specimen mass at various ages. Flexural and compressive strengths were determined according to GB/T 17671-1999, with specimens tested at 7 d, 14 d, and 28 d. Bond strength was measured using an HC-2000A bond strength tester at a loading rate of (5 ± 1) mm/min. XRD was performed using a Bruker D8 diffractometer with a Cu target at a voltage of 40 kV and a current of 40 mA, with a scanning range of 5° to 80° and a step size of 0.02°. For SEM, small sample pieces were dried before observing their morphology; the test was conducted at a current of 0.8 mA and a voltage of 0.22 to 30 kV, and elemental analysis was performed.

3. Results and Discussion

3.1 Physical Properties

3.1.1 Setting Time

Reducing the water-to-binder ratio from 0.55 to 0.40 shortened the initial setting time from 3.8 h to 2.8 h and the final setting time from 7.8 h to 6.8 h, both decreasing consistently with reducing w/b. Loss of fluidity during the initial stage is governed mainly by the rate at which hydration products coat the particle surfaces. At a lower water-to-binder ratio the particles lie closer together and the reaction becomes concentrated, which allows C-S-H gel and ettringite to envelop the particles rapidly, and the paste therefore loses fluidity earlier. Because porosity is low at the final setting stage, gel filling proceeds quickly and hardening shifts to an earlier time. Silica fume accelerated the initial set still further, as its active SiO_2 reacted with calcium hydroxide through the pozzolanic reaction to generate additional gel and improve cohesive bonding, an accelerating behavior consistent with that observed in nano-modified hydraulic lime systems[39, 40].

A final set that arrives too early is unfavorable for internal hydration to proceed to completion. With the SiO_2 nanosol incorporated, final setting was delayed, which gave the hydration products a longer period to form and accumulate and thereby laid the foundation for strength development at later ages. HPMC exerted a dual effect, retarding the initial set while accelerating the final set. The delay stemmed from the water-retention film it forms, which slows the diffusion of free water, whereas the earlier final set is associated with the polymer network bridging particles and hastening the formation of a skeletal framework [41]. Combining the two admixtures balanced operable time against reaction completeness, which supports on-demand control of the setting time of grouting materials. SSPSi and SSPSH thus regulate setting through markedly different mechanisms, one relying on the chemical retardation tied to C-S-H nucleation and the other on physical water retention, a contrast that underpins the

dosage selection in the subsequent work.Fig. 1 gathers the setting times of the ten modified mixes. Initial setting ranged from 3.0 h for SSPSi12.5 0.50 to 3.7 h for SSPSH12.5 0.55, and final setting stayed within 7.1 h to 7.5 h throughout.

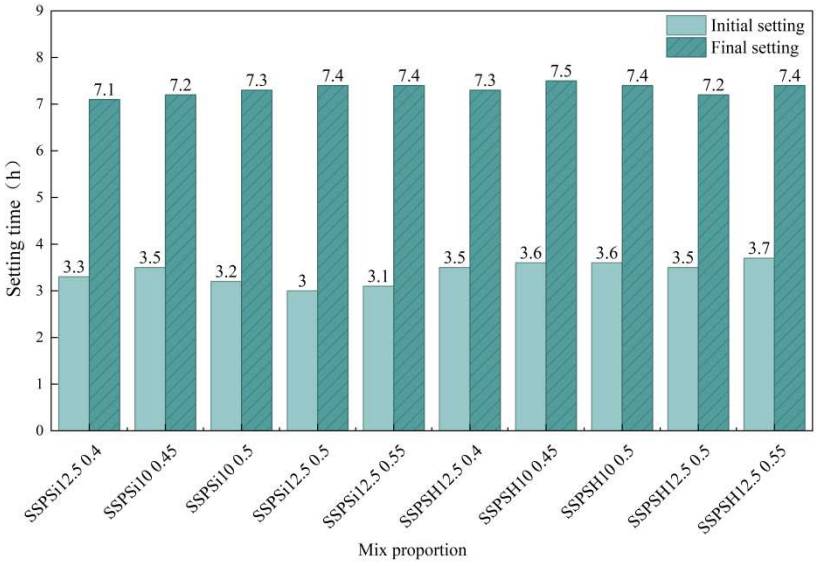


Fig.1 Setting times of modified OSL-based cementitious materials

3.1.2 Fluidity

As Fig. 2a shows, the fluidity of the SSPSi pastes rose with increasing water-to-binder ratio, and SSPSi10 0.50 reached approximately 240 mm. Among the three dosage levels examined, 0.4% proved optimal. A moderate dosage of the SiO_2 nanosol improved particle packing and acted as a lubricant, whereas overdosing triggered agglomeration and a sharp rise in viscosity. Owing to its high specific surface area, nano SiO_2 is highly prone to agglomerate formation once overadded, and such agglomerates deteriorate the rheological behavior of the paste. Scanning electron microscopy showed that the silica sol distributed the lime and silica fume particles more uniformly and filled the voids more completely, in good agreement with the macroscopic fluidity results.

The SSPSH pastes were markedly less flowable overall, as the measurements in Fig. 2b make plain.When silica fume dosages of 12.5% and 15% were combined with the low water-to-binder ratio of 0.40, the flow spread dropped to only 100 to 120 mm.

Raising the HPMC dosage from 0.2% to 0.4% produced little improvement, because the packing effect of the high silica fume fraction and the thickening action of HPMC acted in the same direction and substantially increased the internal frictional resistance of the paste. These findings indicate that for deep fissures where groutability is critical, the SSPSi system should be preferred for deep fissures, or a high-range water-reducing admixture should be co-incorporated to offset the loss of fluidity caused by the HPMC-induced viscosity rise. The contrasting flow responses of the two systems are ultimately the macroscopic manifestation of two distinct modification routes, chemical activation and physical thickening, and this divergence bears directly on their suitability for fractures at different depths, as discussed in the following section.

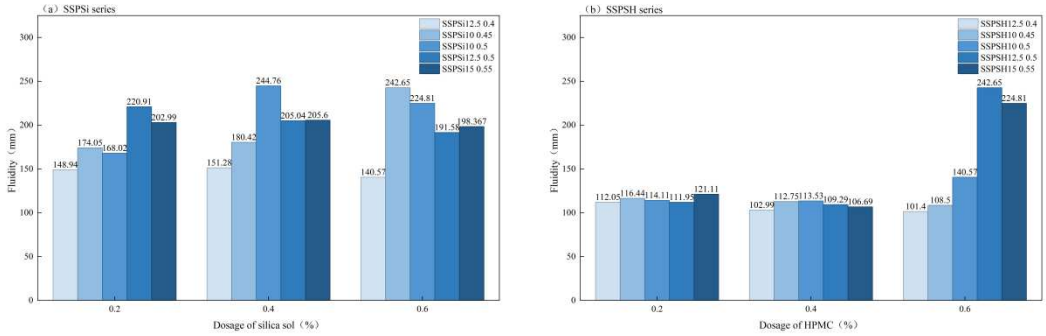


Fig.2 Fluidity of modified OSL-based cementitious materials

3.1.3 Shrinkage

Fig. 3a plots the shrinkage of the SSPSi mixes, and the series showed comparatively high shrinkage at water-to-binder ratios of 0.40 and 0.45. Peak values approaching 0.8% were recorded for SSPSi12.5 0.40 and SSPSi10 0.45, a result attributable to rapid, localized early-age moisture loss. Raising the SiO_2 nanosol dosage to 0.6% brought shrinkage down noticeably, which reflects the micro-filling and densifying action of the nanosilica. Once the water-to-binder ratio was increased to 0.50 and 0.55, SSPSi12.5 0.50 and SSPSi15 0.55 maintained low shrinkage at dosages of both 0.4% and 0.6%.

Across all mixes, the SSPSH series shrank less than the SSPSi series, as the curves

in Fig. 3b confirm.Under low water-to-binder conditions, SSPSH12.5 0.40 and SSPSH10 0.45 containing 0.4% HPMC recorded shrinkage of only 0.2% to 0.3%, the best dimensional stability among all test groups. The uniform water-retaining network formed by HPMC slows moisture evaporation and thereby curbs plastic shrinkage at its source, and this water-retention and shrinkage-reduction mechanism operated through the same pathway reported for cellulose ethers in cement mortars [42]. For lime-based materials that evolve through coupled carbonation and hydration, a stable internal moisture regime is likewise essential to avoid cracking during curing. At higher water-to-binder ratios, the shrinkage of SSPSH15 0.55 increased again to 0.4–0.5%, yet remained below the SSPSi values obtained under identical conditions.

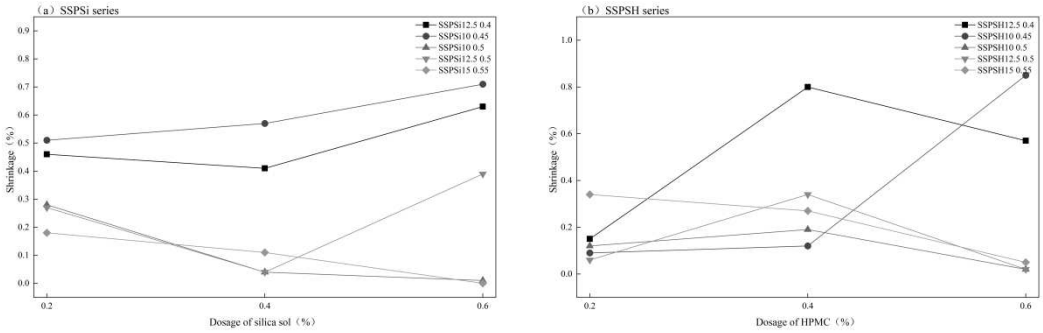


Fig.3 Shrinkage rate of modified OSL-based cementitious materials

3.1.4 Water content and water absorption

As Fig. 4a and Fig. 5a show, the SSPSi series exhibited a water content of 10% to 15% and a water absorption of approximately 45% at a low water to binder ratio. The minimal differences among the three dosages indicate that the micro filling effect of the nano silica sol has refined and sealed the pores. At the intermediate w/b of 0.50, the water content exceeds 20% and the water absorption reaches 50% to 52%. A higher water to binder ratio of 0.55 further elevates the water absorption to approximately 55%. The 0.2% low dosage group exhibits higher values than the 0.4% and 0.6% groups, suggesting that the low concentration silica sol is insufficient to block the interconnected pores formed under high water to binder ratios.

The SSPSH12.5 0.40 group shows a water content of only 5% to 6% in Fig. 4b, ranking the lowest among all groups, which is attributed to the regulation of water migration channels by the HPMC network. Its water absorption of 48% to 50%, plotted in Fig. 5b, is conversely higher than that of the SSPSi series under the same conditions. This indicates that although HPMC promotes uniform water distribution, the microscopic pores of the matrix are not completely filled, resulting in relatively weak impermeability. At medium to high water to binder ratios, the water content and water absorption of SSPSH increase simultaneously. At a dosage of 0.2%, they exceed 30% and approach 65% respectively. At a high water to binder ratio, the SSPSH15 0.55 group experiences a decrease in both values to 18% to 20% and 55% to 57% respectively, benefiting from the synergistic secondary hydration between the HPMC water retention environment and sufficient active SiO_2. The combination of low water content and relatively high water absorption resemble the pore-structure-dependent transport behavior observed in shell aggregate mortar [43]. This suggests that attention should be paid to the filling compactness of shallow fissures during field application.

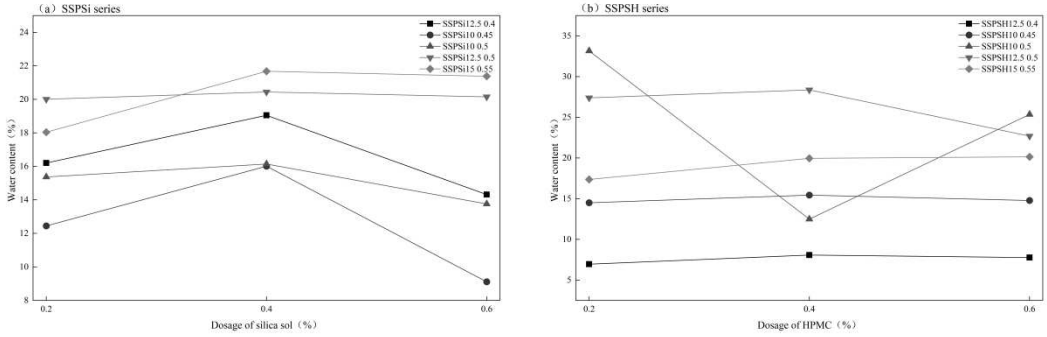


Fig.4 Water content of modified OSL-based cementitious materials

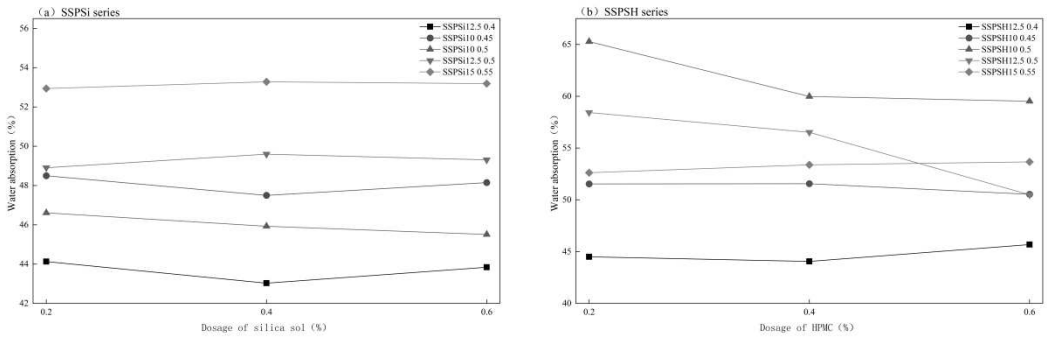


Fig.5 Water absorption of modified OSL-based cementitious materials

3.1.5 Mass change

Fig. 6 tracks the mass of every specimen at 7, 14 and 28 d.At 7 days, the SSPSi series gained mass relatively quickly, with the largest increase recorded at the 0.4% dosage. This behavior follows directly from the penetration of the SiO_2 nanosol into the pore network and the filling of pores by the gel it produces. Mass gain in the HPMC series was slower, most visibly at 0.6%, because the water-retention film retards moisture evaporation and thereby depresses the hydration rate. By 14 days the mass increase had become larger across all groups. SSPSi specimens dosed between 0.4% and 0.6% grew markedly, whereas SSPSi15 0.55 fluctuated as unreacted silica sol accumulated locally, and the 0.4% HPMC group increased steadily over the same interval. At 28 days the groups approached stability. Within the SSPSi system, the 0.4% dosage offered the best stability, while the 0.6% group lost a small amount of mass owing to residual silicate and microcracks. SSPSH likewise performed best at 0.4% dosage, since polymer residues at 0.6% hindered continuous gel growth. Mass change paralleled strength development throughout, which further confirmed 0.4% as the optimal dosage range for both systems.At 28 days the groups approached stability, as the 28 d results in Fig. 6c indicate.

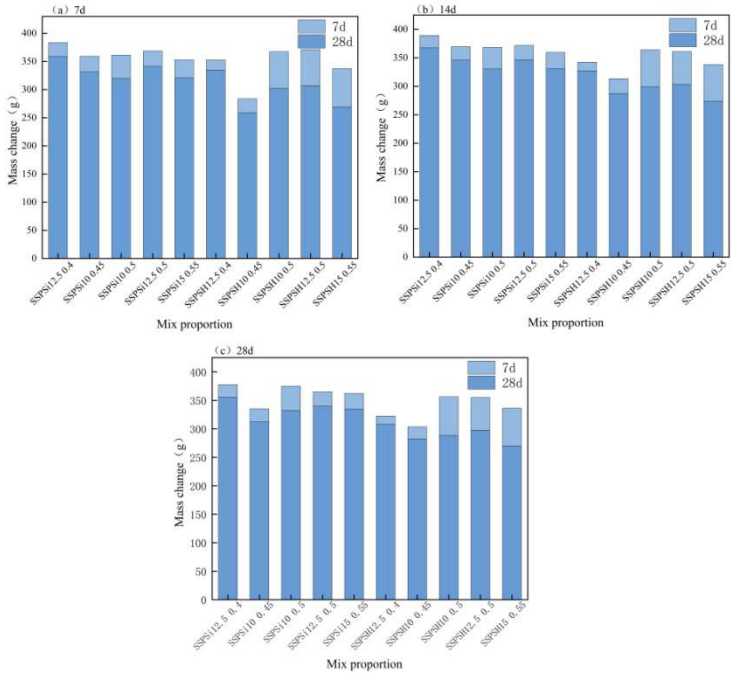


Fig.6 Mass change of modified OSL-based cementitious materials

3.2 Mechanical Properties

3.2.1 Flexural Strength

Flexural strength was generally low in all mixes at 7 days, as the results in Fig. 7a indicate.The SSPSi series held a relative advantage at this age, with SSPSi10 0.45 and SSPSi10 0.50 achieving the highest early-age values, whereas the SSPSH series was weak at early ages and the mix with 0.2% dosage fell to the lowest value among all groups. The two modifiers acted through entirely different pathways at early ages. Reactive SiO_2 began to react pozzolanically with calcium hydroxide as soon as water was added, and the gel promptly filled the capillary pores, so the matrix was already densified in the early stage of curing. The water-retention film of HPMC, by contrast, obstructed the diffusion of free water and thereby delayed hydration.

By 14 days the two series had begun to follow divergent paths, as Fig. 7b shows. SSPSi12.5 0.40 and SSPSi10 0.50 attained their peak values, as the gel by then filled not only the residual pores but also refined the interfacial transition zone. The strengthening of the SSPSH series became visible yet remained modest, because the

gradual release of retained water improved the uniformity of hydration while the thickening effect lowered the packing density, and the two influences largely canceled each other out.

At 28 days, as plotted in Fig. 7c, SSPSi12.5 0.50 attained a peak flexural strength of 1.8 MPa, with SSPSi15 0.55 following at 1.6 MPa, the two highest values among all mixes. In this later stage the physical filling by fine silica fume particles and the chemical reactivity of the SiO_2 nanosol acted synergistically and formed a dense three-dimensional network. The contribution of siliceous pozzolans to the flexural strength of lime-based materials has been well documented in earlier studies [44, 45]. The SSPSH series also increased markedly at 28 days, yet its absolute values remained below those of the SSPSi series, because the polymeric component improved toughness while slightly raising the porosity, and the densification of the matrix was therefore limited.

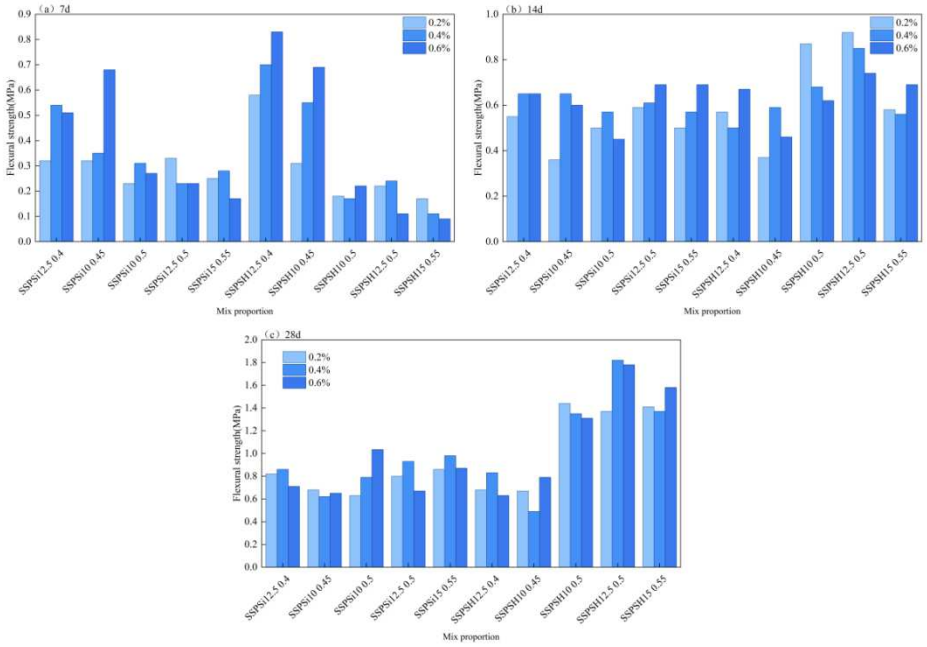


Fig.7 Flexural strength of modified OSL-based cementitious materials

3.2.2 Compressive Strength

At a curing age of 7 days, as Fig. 8a records, the SSPSi12.5 0.40 sample showed the highest compressive strength of approximately 10 MPa at a dosage of 0.2%.When

the dosage increased to 0.6 percent, particularly with SSPSi15 0.55, the accumulation of unreacted siloxane particles led to structural defects and a drop in strength, indicating a clear dosage threshold for nano modification. The SSPSH series showed strengths of only 5 to 7 MPa. By the 14 day mark, as Fig. 8b shows, SSPSi10 0.5 and SSPSi12.5 0.5 approached 9 to 10 MPa, while SSPSH12.5 0.4 reached about 6 MPa. At 28 days, as Fig. 8c shows, SSPSi10 0.5 achieved the peak strength of nearly 11 MPa, followed by SSPSi12.5 0.4 at approximately 10 MPa. The SSPSi15 0.55 mix stayed around 6 MPa, showing the cumulative negative effects of excessive dosage. SSPSH10 0.5 and SSPSH12.5 0.5 measured about 8 MPa and 7 MPa respectively, aided by water release from the HPMC network during later stages that supported continued hydration. Compared with similar modified hydraulic lime grouting materials with a 28 day compressive strength of about 5.4 MPa and the NMK modified NHL system, the optimized formulas in this study show late stage strengths that are similar or higher. Being derived entirely from local shell waste, the optimized mixes offer clear advantages in resource utilization and sustainability [46].

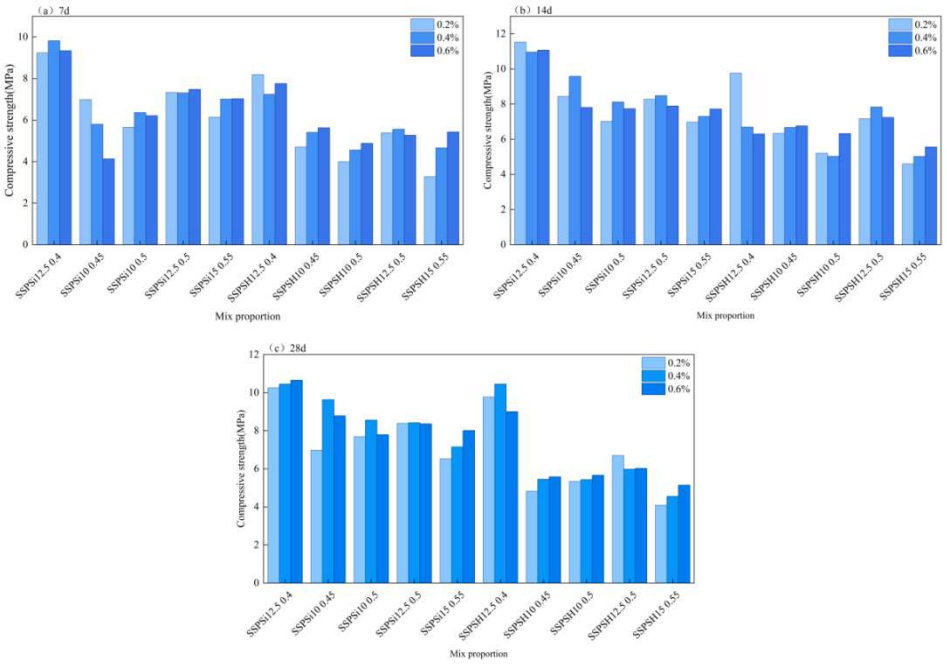


Fig.8 Compressive strength of modified OSL-based cementitious materials

3.2.3 Bond Strength

Fig. 9 compares the bond strength of the four systems at 7, 14 and 28 d. All groups climbed steadily with age, with the most significant growth between 7 and 28 days. At 7 d the SSPSH mix already reached 0.34 MPa while SS stood at 0.12 MPa, and at 14 d the gap widened to 0.60 MPa against 0.18 MPa. By day 28 a distinct gradient had formed, with SSPSH at 0.65 MPa ahead of SSPSi at 0.45 MPa, SSPS at 0.20 MPa and SS at 0.19 MPa.The HPMC system exhibited superior interface bonding performance. This superiority is attributed to the water retention network promoting hydration uniformity in the interface zone, combined with oriented hydration products enhancing mechanical interlocking. Furthermore, the filling of matrix pores and the interface area by gels and AFt provides the physical basis for bond development for this bond development. Interface bonding in grouting materials has historically been a critical weakness in lime-based restoration systems. Previous studies indicate that AMPS water-absorbing resin modified NHL increases bond strength by approximately 12.8%, while NMK modified NHL also significantly enhances both bonding and compressive properties. The increase driven by HPMC in the current system, rising from 0.2 to 0.65 MPa, is comparable to the aforementioned strategies. Notably, this improvement was achieved without introducing any components beyond the synthetic polymer backbone.

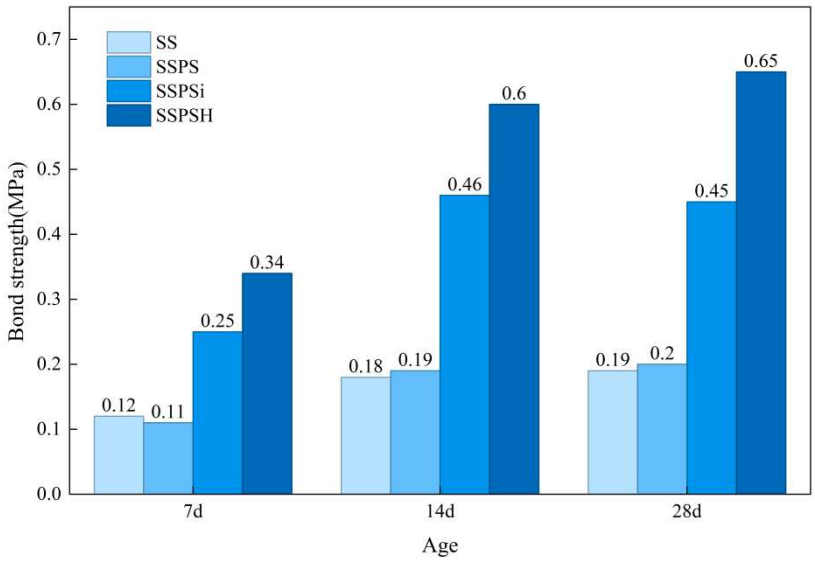


Fig.9 Bond strength of modified OSL-based cementitious materials

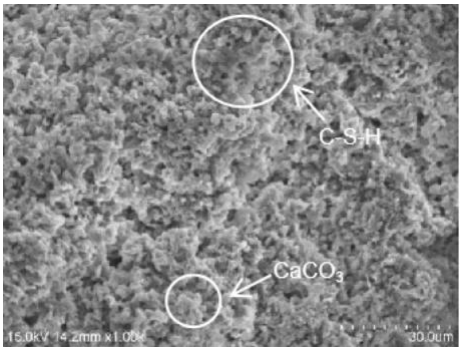
3.3 Microstructural Analysis

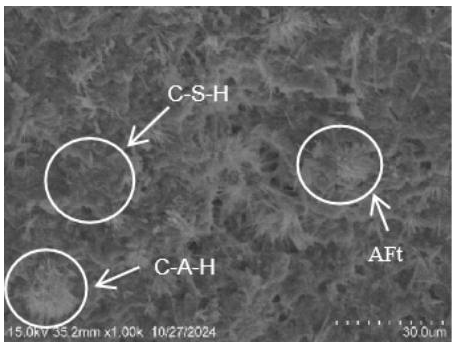
3.3.1 Micromorphology Observation (SEM)

Raising the silica fume content from 10 to 12.5% at a water-to-binder ratio of 0.5, hereafter w/b, markedly increased the formation of C-S-H gel, and the microstructure evolved from a dense and uniform phase into a three-dimensional network of interwoven acicular crystals. The dense gel morphology of the 10% silica fume pastes appears in Fig. 10a and Fig. 10b, and the interwoven acicular network of SSPSi12.5 0.5 0.4 is captured in Fig. 10d.These needle- and rod-like crystals were dominated by AFt and aluminate-bearing hydrates, and the high reactivity of silica fume acted in synergy with silica sol to promote their uniform growth. Needle-shaped hydration products generated by pozzolanic reaction in lime-pozzolan systems have been reported previously, and such three-dimensionally interwoven configurations constitute the microstructural origin of strength and bonding. When the w/b was lowered from 0.5 to 0.4 at 12.5% silica fume and 0.4% silica sol, the morphology transformed into a When the w/b was lowered from 0.5 to 0.4 at 12.5% silica fume and 0.4% silica sol, the morphology transformed into a wrinkled lamellar texture, as Fig. 10c shows, a product

of layer-by-layer C-S-H deposition coupled with hardening shrinkage, and the stacking became increasingly dense, a product of layer-by-layer C-S-H deposition coupled with hardening shrinkage, and the stacking became increasingly dense. Hydration decelerated at the lower w/b, yet the siloxane bond network developed more completely, and combined with the dispersing action of the polycarboxylate superplasticizer, the resistance to cracking and to shrinkage improved in step.

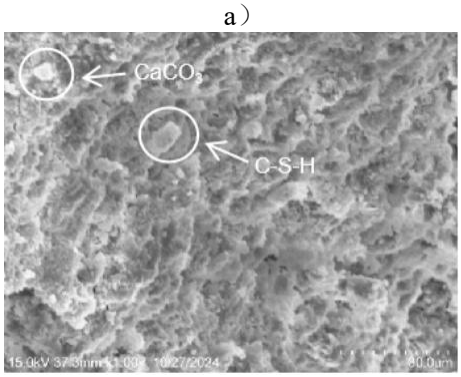
With 0.4% HPMC at a w/b of 0.5, regular cubic products developed in the matrix, as the water-retention film created a stable environment for hydration. Once the w/b decreased to 0.4, a tenderloin-like oriented texture appeared, Once the w/b decreased to 0.4, a tenderloin-like oriented texture appeared, and Fig. 10e shows how the slender strip-shaped hydration products extended along a strongly preferred direction and were well interconnected, so that cracks were effectively dispersed and deflected under load. The polymer-network-induced directional growth observed here is mechanistically analogous to the needle-network bridging architecture that superabsorbent polymers establish in natural hydraulic lime.

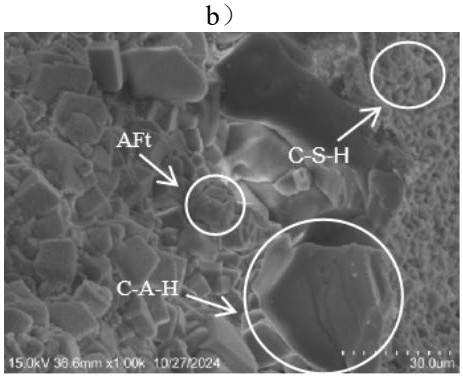




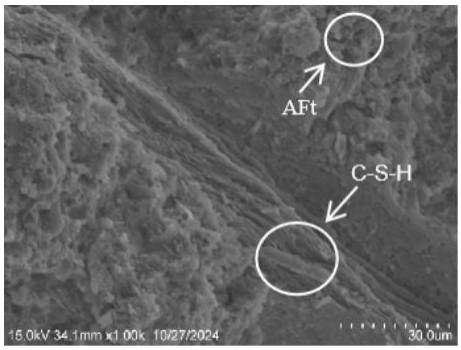
a）

b）





c）　　d）



e）

Fig.10　SEM images of modified OSL-based cementitious materials: a) SSPSi10 0.5 0.2; b) SSPSi10 0.5 0.4; c)SSPSi12.5 0.4 0.4; d) SSPSH12.5 0.5 0.4; e) SSPSH12.5 0.4 0.4

3.3.2 Phase Composition Analysis (XRD)

As Fig. 11 shows, the SSPSi specimens displayed a strong characteristic calcite peak at a 2θ of 29°, which indicates that carbonation dominated their hardening, while the diffuse CSH peaks between 30° and 34° were weak, showing that despite the sufficient activity of the silica sol the consumption of calcium hydroxide remained limited.In the SSPSH specimens, whose patterns also appear in Fig. 11, the calcite peak weakened, which is attributed to HPMC refining the pore structure and hindering the diffusion of CO_2, thereby suppressing excessive carbonation.The carbonation rate of lime based materials is controlled by several factors such as the CO_2 concentration, the water to binder ratio and the admixtures [47, 48], and the size and development of calcite crystals are directly linked to the macroscopic strength. The moderate suppression of carbonation by SSPSH in this system balances the early hydration strength against long-term densification through carbonation.

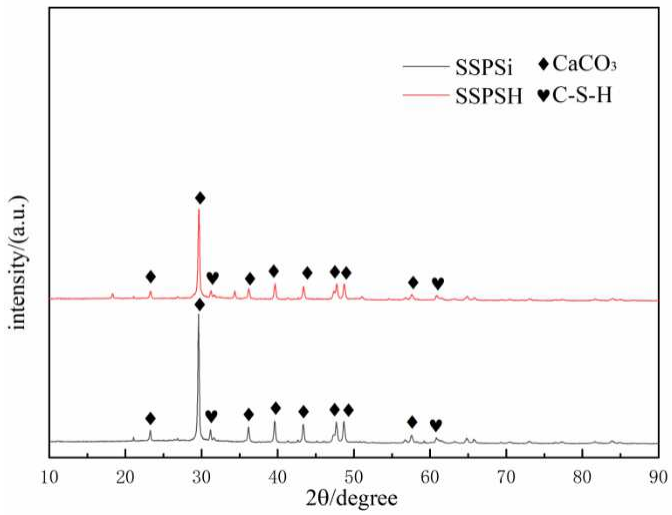


Fig.11 XRD patterns of modified OSL-based cementitious materials

3.4 Laboratory Simulation and Field Verification of Fissure Grouting Repair

3.4.1 Fissure Investigation and Laboratory Grouting Simulation

The Yuewang Temple sits in a subtropical monsoon climate where the annual mean relative humidity ranges from 70% and 80%, and its stone relics have long served in the open air. Under such humid conditions, the repeated crystallization of soluble salts ranks among the principal drivers of deterioration in exposed stone relics[49], and the compatibility demands placed on repair materials themselves, low soluble salt content, low shrinkage and moderate strength, thus become more prominent[50].

The field survey documented 70 cracks in total. Of these, 52, or 74%, ran 40 to 70 mm deep and clustered on the railings beside the tomb, the base of the tomb stele, the stone figures and animals along the tomb passage, and the surfaces of stone steles. Deep and shallow fissures coexist, with medium and deep cracks prevailing, so a single mix proportion can hardly serve both, and that mismatch was the direct motivation for the present study of crack depth and mix selection.

In the laboratory, cementitious cubes of 100 mm side length served as surrogates

for the stone substrate, and the intact controls reached 41.2 MPa in compression at 28 days. Guided by the survey findings, we prefabricated through-thickness cracks with depths of 40, 50, 60 and 70 mm deep were prefabricated, and measured grout volumes of 20, 25, 30 and 35 mL were injected into the 40, 50, 60 and 70 mm cracks respectively. Each group contained three replicate specimens. After 28 days of curing at 20 ± 2 °C and 70% to 80% relative humidity, the cubes were tested for compressive strength, and the results are given in Table 4.

Among the four mixes, SSPSi12.5 0.50 0.4 recorded the highest strength in every depth interval, and its strength fell by only 16.1% as the crack deepened from 40 to 70 mm, while recovery relative to the intact substrate ranged from 68% to 82%. The two SSPSH mixes lost more than 37%, and at 60 mm and deeper their recovery stayed below 51%. The contrast in decay mirrors the flowability gap between the two systems. At a water-to-binder ratio of 0.50 the SSPSi grout reached a fluidity of roughly 240 mm and filled the deep cracks thoroughly, whereas the SSPSH series, thickened by HPMC and therefore subject to high internal friction, left deep fissures partly unfilled, and these voids acted as weak planes under load, magnifying the strength loss.

Table 4 Compressive strength and recovery rate of grouted specimens (MPa)

Mix proportion	40 mm	50 mm	60 mm	70 mm
SSPSi12.5-0.40-0.4	25.4 (62%)	23.9 (58%)	24.8 (60%)	23.4 (57%)
SSPSi12.5-0.50-0.4	33.4 (81%)	33.7 (82%)	30.1 (73%)	28.0 (68%)
SSPSH12.5-0.40-0.4	20.8 (50%)	20.6 (50%)	17.5 (42%)	13.1 (32%)
SSPSH12.5-0.50-0.4	28.4 (69%)	25.3 (61%)	20.7 (50%)	17.8 (43%)

Note: Values in parentheses represent the strength recovery rate relative to the intact specimen (41.2 MPa)

At the same time, the laboratory results revealed another side of the comparison. Across the 40 to 50 mm shallow zone, SSPSH12.5 0.50 0.4 attained a recovery rate of 61% to 69%, and its 28 d bond strength of 0.65 MPa, together with shrinkage held within 0.2% to 0.3%, ranked first among all mix proportions tested. Repairs of shallow

fissures failed mainly through interfacial debonding and surface cracking rather than through inadequate bearing capacity, which made interfacial adhesion and crack resistance the dominant requirements. Surrendering the low shrinkage and high bond of SSPSH in exchange for a deep injectability that such repairs would never call upon was therefore unnecessary. On balance, the selection criterion was set as SSPSi12.5 0.50 0.4 for fissures deeper than 50 mm, and SSPSH12.5 0.50 0.4 for shallow fissures within 40 to 50 mm.

At the site, grouting began with the deepest fissures and proceeded toward the shallower ones. Each fissure was rinsed with deionized water and dried, after which a slurry of the same mix proportion sealed the exposed surface while grout injection ports were reserved for injection. A small grouting pump then delivered the material in stages, with every lift kept to no more than 5 cm and separated from the next by 24 h. After curing, the nozzles were removed and the joints were repointed, and lime slurry was applied to give the repairs an aged appearance in keeping with the relic.

Inspection 28 d after grouting showed the fissures densely filled and effectively closed, the hardened grout firmly bonded to the limestone body, and no shrinkage cracking or interfacial debonding anywhere in the treated area. Once the aged finish was in place, the repaired zones blended coherently with the original appearance of the relic. These field observations bore out the laboratory strength data, and the criterion linking fissure depth to mix selection thereby completed its transfer from the laboratory to the heritage substrate.

In recent years, microbially induced calcium carbonate precipitation, or MICP, has been validated for field consolidation of sandstone cultural relics[51], and nanomodified lime mortar has likewise completed field application at the Yungang Grottoes. Measured against these approaches, the material developed here uses waste oyster shells gathered locally as its sole base material and introduces neither soluble salts nor foreign cementitious components, so it achieves a more favorable balance among repair performance, cost, and the principle of using locally available materials. It can therefore

be extended directly to the fissure repair of limestone cultural relics in comparable coastal environments of high humidity.

4. Conclusions

Calcined oyster shell lime from Sanmen, Zhejiang Province, was used as the sole binder in this study. Small amounts of silica fume and superplasticizer were incorporated, after which silica sol or hydroxypropyl methylcellulose was added to prepare two modified grouts for repairing cracks in limestone relics exposed to humid coastal environments. Based on laboratory tests, microstructural observations, and a field repair at the Yuewang Temple in Hangzhou, the following conclusions can be drawn:

(1) Reducing the water-to-binder ratio from 0.55 to 0.40 shortened the initial and final setting times by approximately 1 h. Silica sol delayed the final setting and thus prolonged the hydration period, whereas HPMC delayed the initial setting but accelerated the final setting. The paste exhibited the best fluidity, with a spread of approximately 240 mm, at a silica sol dosage of 0.4%; the paste containing HPMC was noticeably more viscous and therefore exhibited poorer injectability.

(2) At a silica sol dosage of 0.4%, the 28-day compressive and flexural strengths of the grout reached 10.9 MPa and 1.8 MPa, respectively. Increasing the dosage to 0.6% reduced rather than increased the strength, because excess particles agglomerated and acted as defect sites. The HPMC-modified grout attained a 28-day compressive strength of approximately 8 MPa, but its shrinkage was only 0.2%–0.3%, and its bond strength increased from 0.2 MPa for the reference paste to 0.65 MPa. The two admixtures thus play complementary roles: silica sol provides higher strength, whereas HPMC combines low shrinkage with strong adhesion.

(3) In the silica sol-modified grout, abundant acicular and rod-like ettringite crystals interwove into a supporting skeleton, while the remaining pores were filled with calcium silicate hydrate gel; this microstructure accounts for the higher strength.

In the HPMC-modified grout, the hydration products grew preferentially in a single direction into elongated slender fibers. Moreover, HPMC retarded the inward diffusion of CO_2 and thereby prevented excessively rapid carbonation, which contributed to its strong adhesion and low shrinkage.

(4) Both the laboratory grouting simulation and the field repair at the Yuewang Temple in Hangzhou confirmed that the grouts bonded firmly to the limestone, and no cracking or interfacial debonding occurred after hardening. The on-site bond strengths reached 80%–88% of the laboratory values, and after artificial aging, the appearance of the repaired areas was essentially consistent with that of the original relic substrate.

(5) Based on the combined performance of the two grouts in terms of injectability, strength, and adhesion, a crack-depth-based selection guideline is proposed: cracks deeper than 50 mm should be filled with SSPSi12.5-0.50-0.4, which offers good injectability and higher strength, whereas shallow cracks of 40–50 mm should be filled with SSPSH12.5-0.50-0.4, which exhibits lower shrinkage and better adhesion. This guideline has been verified through field application and can be applied directly to the crack repair of similar limestone relics in coastal environments.

It should be noted that this study evaluated only the short-term performance of the grouts cured for up to 28 d under standard conditions. Future research will investigate the long-term durability of the grouts under wetting–drying cycles, salt crystallization, and freeze–thaw cycles, and compare the carbon emissions of oyster shell lime with those of commercial natural hydraulic lime.

References

[1]Suchy,H.,P.Zalar,and M.F.Macedo,Microbial Diversity of Biodeteriorated Limestone Cultural Heritage Assets Identified Using Molecular Approaches—A Literature Review.Applied Sciences,2024.14(16).

[2]Sesana,E.,et al.,Climate change impacts on cultural heritage:A literature review.WIREs Climate Change,2021.12(4).

[3]Reboah,P.,et al.,The biological contribution to the weathering of limestone monuments in a vegetated urban area:results of a 5-year exposure.Heritage Science,2024.12(1).

[4]Veiga,R.,Air lime mortars:What else do we need to know to apply them in conservation and rehabilitation interventions?A review.Construction and Building Materials,2017.157:132-140.
[5]Chen,Z.,et al.,A review of mechanical properties and carbonation behavior evolution of lime mortar for architectural heritages restoration.Minerals and Mineral Materials,2024.3(1).
[6]Shi Pei,He.,Ma Tao,et al.,“Study on the Hydration Behavior and Performance of Natural Hydraulic Lime Cured in Montmorillonite.”Journal of Chongqing University,2024,47:96–102.
[7]Wang Zhenbo,Meng.,Liu Ze,et al.,Mechanical Properties of High-Ductility Natural Hydraulic Lime-Based Materials.Journal of Building Materials,2024.27:1143–1151.
[8]et al.,Cui,Fang,Zhou.“A Comparative Study on the Properties of Hydraulic Lime H•C5 and NHL5 as New Grouting Materials for Cracks in Grotto Temples.”Journal of Northwest Normal University(Natural Science Edition),2025,61:36–44.
[9]Li Xin,Shao Mingshen,Guo Hong,et al.,“A Study on the Laboratory Comparison of Grouting Materials for Hollow Areas in the Meidai Zha Murals in Inner Mongolia.”Research on the Conservation of Grottoes and Earthen Sites,2025,vol.4,38–50.
[10]Sarcinella,A.and M.Frigione,Phase Change Materials in Lime-Based Mortars for the Energy Efficiency of Historic Buildings:State-of-the-Art and Prospects.Coatings,2026.16(7).
[11]Fernández,J.M.,et al.,Influence of nanosilica and a polycarboxylate ether superplasticizer on the performance of lime mortars.Cement and Concrete Research,2013.43:12-24.
[12]Al-Mulali,M.Z.,et al.,Performance Analysis of Cement Mortar Modified with Nano-Silica and Nano-Alumina.Buildings,2026.16(5).
[13]Chen,N.,et al.,Water Retention Mechanism of HPMC in Cement Mortar.Materials,2020.13(13).
[14]Shao Mingshen,Li,Zhang.“Oyster Shell Lime in Ancient Chinese Architecture and Its Basic Properties.”Research on Chinese Cultural Relics,2015:91–96.
[15].Li Zuxiong,Z.L.,Wang Jinua,Research on the modification of two traditional building materials in ancient China.Heritage Science,2013.
[16]Shao,M.,et al.,Investigation and modification of two kinds of Chinese traditional lime in cultural building relics.Journal of Cultural Heritage,2019.36:118-127.
[17]Chen,W.,et al.,Modification of traditional Chinese ginger nut and its mechanical behavior.Construction and Building Materials,2017.144:138-146.
[18]Zhang,Z.-j.,et al.,Experimental study on factors affecting the physical and mechanical properties of shell lime mortar.Construction and Building Materials,2019.228.
[19]Mo,K.H.,et al.,Recycling of seashell waste in concrete:A review.Construction and Building Materials,2018.162:751-764.
[20]Tayeh,B.A.,et al.,Properties of concrete containing recycled seashells as cement partial replacement:A review.Journal of Cleaner Production,2019.237.
[21]Eziefula,U.G.,J.C.Ezeh,and B.I.Eziefula,Properties of seashell aggregate concrete:A review.Construction and Building Materials,2018.192:287-300.
[22]Hamada,H.M.,et al.,Effect of recycled seashells on concrete properties:A comprehensive review of the recent studies.Construction and Building Materials,2023.376.
[23]Jasni,S.A.,et al.,Use of Seashell as Cement Replacement in Construction Material:A Review.Construction,2024.4(1):7-20.

[24]Liao,Y.,et al.,Experiment research on effect of oyster shell particle size on mortar transmission properties.Construction and Building Materials,2023.375.
[25]Luo,K.,et al.,Evaluation of using oyster shell as a complete replacement for aggregate to make eco-friendly concrete.Journal of Building Engineering,2024.84.
[26]Oh,S.-E.,et al.,Comparative analysis of the effects of waste shell aggregates on the material properties of cement mortars.Construction and Building Materials,2024.412.
[27]Terzić,A.,et al.,Green Materials for Cement Clinker:Assessing Alternative Raw Material Potential.Materials,2026.19(4).
[28]Ho Viet,T.,P.Tran Thi Thanh,and Q.Le Thi Ngoc,Partial replacement of natural sand with recycled waste oyster shells in concrete production of grade 30 MPA.Journal of Materials&Construction,2026.16(01).
[29]Chen,W.and L.Li,A new ingredient to improve Chinese traditional hydraulic lime and its assessment on stone heritage conservation.Heritage Science,2024.12(1).
[30]BELLEI P,S.G.,MAGALHÃES F,et al,Oyster shells'incorporation into mortar to achieve blue circular economy—LCA case study in Portugal.Procedia Structural Integrity,2024.55:96-102.
[31]Eires,R.,et al.,Calcium-Based Wastes as Additives or Binder Substitutes in Mortars:Experimental Research with Oyster Shells or Lime Kiln Dust,Quicklime and a Modified Vinegar Solution.Construction Materials,2026.6(1).
[32]Travincas,R.,et al.,Performance and Accelerated Ageing of an Industrial Hydraulic Lime Mortar Applied on Different Substrates.Coatings,2024.14(7).
[33]Ma Qinglin,Xu.,"Research Progress on Natural Hydraulic Lime-Based Mortars for the Restoration of Historic Buildings." Research on the Conservation of Grottoes and Earthen Sites,2022.
[34]Feng,S.and S.Guan,Influence of nano-SiO2 and nano-TiO2 on early hydration process of cement:Hydration rate,hydration products microstructure,calcium ion solubility,and diffusion ability.Construction and Building Materials,2025.491.
[35]Hwang,Y.,S.Woo,and Y.-C.Choi,Effect of Synthesized C-S-H Nanoparticles on the Early Hydration and Microstructure of Cement.Materials,2025.18(14).
[36]Geng,Z.,et al.,Effect of Nano-SiO2 on the Hydration,Microstructure,and Mechanical Performances of Solid Waste-Based Cementitious Materials.Materials,2025.18(11).
[37]Malathy,R.,et al.,Mechanical and Microstructural Properties of Composite Mortars with Lime,Silica Fume and Rice Husk Ash.Processes,2022.10(7).
[38]Wang,X.,et al.,Effect of biological shells aggregate on the mechanical properties and sustainability of concrete.Scientific Reports,2024.14(1).
[39]Ji,Y.,et al.,Performance evaluation and application of nano-metakaolin modified natural hydraulic lime for stone cultural heritage restoration.npj Heritage Science,2025.13(1).
[40]Zhu,Z.,et al.,Effects of nano-metakaolin on the enhanced properties and microstructure development of natural hydraulic lime.Chinese Chemical Letters,2025.36(4).
[41]et al.,Liu,Chai,Li."Effect of In-Situ Polymerization of AMPS Water-Absorbing Resin-Modified Natural Hydraulic Lime on the Grouting Performance in Sandstone Fractures." Journal of Chongqing University,2024,47:172–180.

[42]Silva,A.L.d.,E.R.Kohlman Rabbani,and M.Shakouri,Seashell Powder as a Sustainable Alternative in Cement-Based Materials:A Systematic Literature Review.Sustainability,2025.17(2).
[43]Martínez-García,C.,et al.,Mussel shell mortars durability:Study of aggregate replacement limit.Journal of Building Engineering,2024.82.
[44]Tayeh,B.A.,et al.,Durability and mechanical properties of seashell partially-replaced cement.Journal of Building Engineering,2020.31.
[45]Koteng,D.O.and C.-T.Chen,Strength development of lime–pozzolana pastes with silica fume and fly ash.Construction and Building Materials,2015.84:294-300.
[46]Hasan,K.,et al.,A review of the mechanical properties and durability of concrete containing recycled seashells as a partial cement replacement.Journal of Material Cycles and Waste Management,2023.25(6):3192-3216.
[47]Silva,B.A.,et al.,Effects of natural and accelerated carbonation on the properties of lime-based materials.Journal of CO2 Utilization,2021.49.
[48]Ergenç,D.and R.Fort,Accelerating carbonation in lime-based mortar in high CO2 environments.Construction and Building Materials,2018.188:314-325.
[49]Zhang Liangshuai,Wang.,Jia Yiming et al.,“Mechanisms of Salt-Induced Deterioration of Stone Cultural Artefacts Exposed to Humid Environments.” Journal of Chongqing University,2024,47(10):86–98.
[50]Sena da Fonseca,B.,Current Trends in Stone Consolidation Research:An Overview and Discussion.Buildings,2023.13(2).
[51]Li,J.,et al.,Consolidation of sandstone built heritage by EICP and MICP:Evaluation of laboratory and in situ application.Construction and Building Materials,2025.489.

Dual Modified Calcined Oyster Shell Lime Grouts for Crack Repair in Humid Coastal Limestone Relics

Yongguo Chen[a,b], Miaodan He[a], Jinyao Ye[a],Liang Ye[a,b,*], Shusheng Shen[a,b,*], Sheng Ye[c], Zixuan Chen[d],Jinjing Chen[a], Ruiqi Zhang[a],Zhen Wang[a], Yingzi Huang[a] and Yi Chen[a]

[a] School of Civil Engineering and Architecture, Zhejiang University of Science and Technology, Hangzhou 310023, China

[b] Zhejiang–Singapore Joint Laboratory for Urban Renewal and Future City, Hangzhou 310023, China

[c] Yue Temple Management Office of Hangzhou West Lake Scenic Area, Hangzhou 310000, China

[d] School of Architecture, Tianjin University, Tianjin 300072, China

* Corresponding authors.

Liang Ye, School of Civil Engineering and Architecture, Zhejiang University of Science and Technology, No. 318 Liuhe Road, Hangzhou 310023, China. E-mail: liangye662162@163.com

Shusheng Shen, School of Civil Engineering and Architecture, Zhejiang University of Science and Technology, No. 318 Liuhe Road, Hangzhou 310023, China. E-mail: shushengshen014@163.com

E-mail addresses

Y. Chen: 108016@zust.edu.cn; Y. Huang: 212502833008@zust.edu.cn;

J.Chen:222502859028@zust.edu.cn;Z. Chen: Zixuanchen0866@163.com; R. Zhang: RuiqiZhang7962@163.com; Z. Wang: Zhenwang8863@163.com; J. Ye: jinyaoye8687@163.com; Y. Chen: yichen5748@163.com; M.He:15957950435@163.com;S.Ye:yeshen5216@163.com

Corresponding Author

liangye662162@163.com;shushengshen014@163.com

CRediT author statement

Yongguo Chen: Conceptualization, Funding acquisition, Project administration, Writing – review & editing.

Miaodan He: Validation.

Jinyao Ye: Validation, Formal analysis.

Liang Ye: Data curation, Supervision, Validation, Writing – review & editing.

Shusheng Shen: Supervision, Validation, Project administration.

Sheng Ye: Investigation, Resources.

Zixuan Chen: Visualization, Software

Jinjing Chen: Investigation

Ruiqi Zhang: Investigation, Data curation, Resources

Zhen Wang: Investigation, Software

Yingzi Huang: Conceptualization, Methodology, Software, Formal analysis, Visualization, Writing – original draft

Yi Chen: Validation, Investigation

Funding

This work was supported by the Zhejiang Province Leading Geese Plan (Grant No. 2024C03261); the project "Investigation and Analysis of the Characteristics of Cliff Stone-Carving Deterioration in the Wenzhou Area" (Grant No. 2025018); the Zhejiang University of Science and Technology Graduate Research and Innovation Fund (Grant No. 2024yjskc10); the Zhejiang University of Science and Technology Graduate Teaching Reform Project (Grant No. 2024yjsjg04); and the Zhejiang University of Science and Technology Undergraduate Teaching Reform Project (Grant No. 2025-ksj2).

Declaration of competing interest

The authors declare that they have no known competing financial interests or personal relationships that could have appeared to influence the work reported in this paper.

Declaration of generative AI and AI-assisted technologies in the writing process

The authors declare that no generative AI or AI-assisted technologies were used in the writing process of this work.